WORLD JOURNAL OF PHARMACY AND PHARMACEUTICAL SCIENCES
SJIF Impact Factor 6.647
Volume 6, Issue 8, 1189-1201 Research Article ISSN 2278 – 4357

CHARACTERIZATION OF Mg DOPED ZnO NANOPARTICLES SYNTHESIZED BY A NOVEL GREEN ROUTE USING *AZADIRACHTA INDICA* GUM AND ITS ANTIBACTERIAL ACTIVITY

A. Geetha[1], R. Sakthivel[2] and J. Mallika[1]*

[1]Research Scholar, Department of Chemistry, PSG College of Arts and Science, Coimbatore, Tamil Nadu, India-641014.

[1*]Assistant Professor, Department of Chemistry, PSG College of Arts and Science, Coimbatore, Tamil Nadu, India-641014.

[2]Associate Professor, Department of Electronics, PSG College of Arts and Science, Coimbatore, Tamil Nadu, India -641014.

Article Received on
27 May 2017,

Revised on 16 June 2017,
Accepted on 06 July 2017

DOI: 10.20959/wjpps20178-9719

***Corresponding Author**
Dr. J. Mallika
Assistant Professor, Department of Chemistry, PSG College of Arts and Science, Coimbatore, Tamil Nadu, India-641014.

ABSTRACT

Eliminating the use, generation of materials hazardous to human health and the environment, green synthesis using plants have been proposed as an alternative and environmentally friendly methods in the synthesis of metallic nanoparticles. The present work deals with the green synthesis of Mg-doped ZnO nanoparticles using *Azadirachta indica* gum as bio template. X-Ray diffraction patterns of the prepared nanoparticles confirmed the hexagonal wurtzite structure and the crystallite size decreases as the doping concentration of Mg increases. Field Emission Scanning Electron Microscope (FE-SEM) confirms the presence of flower-like structure. Energy Dispersive X-ray (EDAX) result confirms the presence of zinc, oxygen and Mg atoms and proves that the dopant Mg has successfully incorporated into the ZnO matrix. From the UV-Vis absorption spectra, the band gap energy of the Mg doped ZnO nanoparticles was calculated and found to increase with the increase in Mg concentration. The antibacterial activity of the Mg doped ZnO samples on gram positive *S. aureus* and gram negative *E.coli* bacterial strains was assayed by well diffusion method.

KEYWORDS: *Azadirachta indica, S. aureus, E.coli.*

1. INTRODUCTION

Nanobiotechnology is an emerging field, which has revolutionized each and every field of science. Medical, pharmaceutical, agricultural and environmental sciences are some fields where nanostructures have a wide application.[1] Zinc oxide, with its unique physical and chemical properties, such as high chemical stability, high electrochemical coupling coefficient, a broad range of radiation absorption and high photostability, is a multifunctional material.[2] A semiconductor nanoparticle such as ZnO, TiO_2 and SiO_2 has become the centre of attention due to their unique optical, electronic, structural and catalytic properties.[3] Among this, ZnO nanoparticles with a wide direct band gap (3.37eV) and a large excitonic binding energy (60meV) have larger applications.[4] It has a wide application in rubber industry, pharmaceutical and cosmetic industry, textile industry, electronic and electro technology and photocatalysis. Zinc oxide nanoparticles play a role in promoting seed germination, seedling vigour and plant growth.[5] Zinc oxide nanoparticles showed antibacterial activity against various organisms.[6,7] The doping of ZnO nanoparticles showed more antibacterial activity than the pure ZnO nanoparticles.[8] Doping of MgO to ZnO has a wider band gap of 7.3eV.[9] The antibacterial activities of Mg-doped ZnO nanoparticles synthesized by a simple co-precipitation technique have been investigated against bacterial strains. It has been interestingly observed that Mg-doping has enhanced the inhibitory activity of ZnO against *S. aureus* more efficiently than the *E. coli* bacterial strain.[10] The antibacterial activity of the nanoparticles was tested against *E.coli* (Gram-negative bacteria) cultures and was found that both pure and doped ZnO nanosuspensions show good antibacterial activity.[11] The earlier literature survey suggests that various gum exudates such as gum *olibanum*, gum *arabic*, and gum *kondagogu* and gum *karaya* have been reported as reducing and stabilizing agent for the synthesis of gold, silver and copper nanoparticles.[12-16]

Azadirachta indica gum obtained from neem tree is a natural polysaccharide, is widely utilized as emulsifier, thickener, and stabilizer due to its stability in a wide range of pH and temperature and high viscosity. In the present study, we have reported the green synthesis of Mg doped ZnO nanoparticles using *Azadirachta indica* gum as the stabilizing agent (bio template). The synthesized nanoparticles were characterized using UV-Vis, FT-IR, XRD, EDAX and FE-SEM techniques.

2. MATERIALS AND METHODS

2.1. Materials

Zinc nitrate hexahydrate, magnesium nitrate hexahydrate, and sodium hydroxide were purchased from Merck Chemicals with 99% purity. *Azadirachta indica* gum used in the present work was collected locally from the barks of the neem tree and purified using double distilled water.[17,18]

2.2. Green synthesis of Mg-doped ZnO nanoparticles

High purity Mg-doped ZnO nanoparticles were synthesized using a simple wet chemical method. About 1 g of zinc nitrate was dissolved in 90 ml of double distilled water. After 10 minutes stirring, about 0.1 g of AI gum in 10 ml water was added. To this mixture, stoichiometric quantities of magnesium nitrate solution calculated using the formula $Zn_{1-x}Mg_xO$ (where x=0.0, 0.01, 0.03 and 0.05) was added. Then, about 100 ml of NaOH solution was added dropwise with vigorous stirring for 3 hours. The white suspension obtained was centrifuged and dried in hot air oven at 80^{o}C. The white crystalline powder of Mg doped ZnO was obtained.

2.3. Characterization techniques

The UV-Visible absorption spectra of undoped and Mg-doped ZnO nanoparticles were recorded using JASCO Corp., V-570 spectrophotometer over a range of 200-800 nm. The presence and interaction of chemical functional groups of the prepared nanoparticles were analyzed using FT-IR spectrophotometer (Perkin Elmer) at the scanning range of 400-4000 cm^{-1}. The X-Ray powder diffraction patterns were recorded using an X-Ray diffractometer (XRD, PW 3040/60 Philips) with Cu (kα) radiation (λ=1.5406 A$^{\circ}$) operating at 40 kV and 30 mA with 2θ ranging from 20°- 90°. The surface morphology of Mg-doped ZnO nanoparticles was characterized by using FE-SEM. The antibacterial activity was also investigated using well disc diffusion method. Two pathogenic bacterial strains namely *E. coli* and *S. aureus* were used in this investigation.

2.4 Antibacterial assay

The antibacterial activity of the Mg doped ZnO samples on gram positive *S. aureus* and gram negative *E.coli* bacterial strains was assayed by the well diffusion method. The effect of the given sample can be assessed by the inhibition of mycelia growth of the bacteria and was observed as a zone of inhibition near the wells. Muller Hinton agar was prepared and sterilized. Log phase culture of the test specimens was swabbed over the agar surface using

the sterile cotton swab and about 10 µl of the given samples were loaded onto the wells. The plates were incubated at 37^0 C for 24 hours. The incubated plates were examined for the interruption of growth sample. The zone of inhibition was calculated by measuring the diameter of the inhibited growth around the substrate.

RESULTS AND DISCUSSION

3.1. UV-Visible absorption spectra

The UV-Vis absorption spectra of pure ZnO and Mg doped ZnO ($Zn_{0.97}Mg_{0.03}O$, $Zn_{0.95}Mg_{0.05}O$, and $Zn_{0.93}Mg_{0.07}O$) synthesized using AI gum as the bio-template are given in Figures 1 and 2.

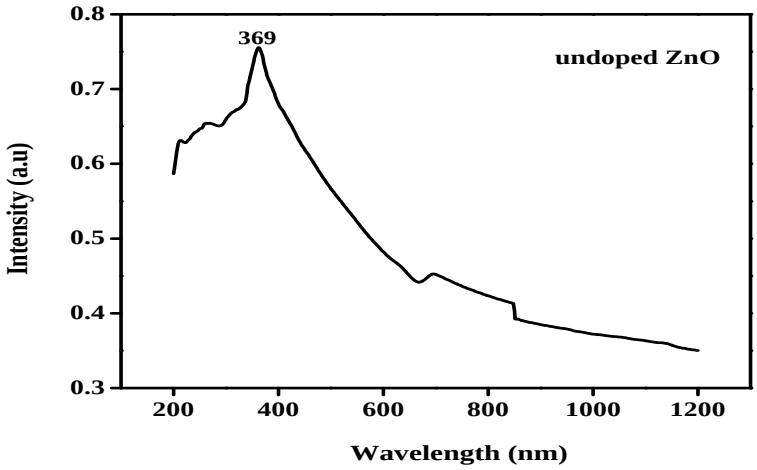

Figure 1: UV-Visible absorption spectra of undoped ZnO using AI gum as bio-template.

UV-Visible absorption spectroscopy is highly useful to investigate the effect of doping on optical properties of nanoparticles. The absorption edge of undoped ZnO is 369 nm. The addition of Mg as dopant shifts the absorption wavelength towards the lower side. The absorption wavelength of $Zn_{0.97}Mg_{0.03}O$, $Zn_{0.95}Mg_{0.05}O$, and $Zn_{0.93}Mg_{0.07}O$ nanoparticles are 355, 352, and 348 nm respectively. This indicates the stronger interaction between the dopant and the ZnO nanoparticles. The intensity of absorption also increases with increase in the concentration of dopant. Band gap energies of the synthesized nanoparticles were calculated by the following relation[17],

$E_g = (1240/\lambda)$ eV

λ- Wavelength of nanoparticles

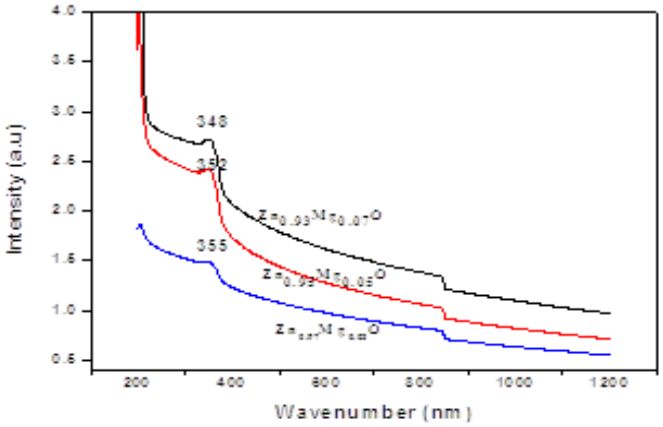

Figure.2 UV-Visible absorption spectra of green synthesized Mg-doped ZnO using AI gum as stabilizing agent.

The absorption wavelength and band gap energy of the undoped ZnO, $Zn_{0.97}Mg_{0.03}O$, $Zn_{0.95}Mg_{0.05}O$ and $Zn_{0.93}Mg_{0.07}O$ nanoparticles are included in Table.1.

Table 1: Absorption wavelength and band gap energy of (a) ZnO, (b) $Zn_{0.97}Mg_{0.03}O$, (c) $Zn_{0.95}Mg_{0.05}O$ and (d) $Zn_{0.93}Mg_{0.07}O$.

S.No	Composition	Wavelength (nm)	Band gap energy eV
1	ZnO	369	3.36
2	$Zn_{0.97}Mg_{0.03}O$	355	3.49
3	$Zn_{0.95}Mg_{0.05}O$	352	3.52
4	$Zn_{0.93}Mg_{0.07}O$	348	3.56

The band gap energies of the synthesized nanoparticles are found be 3.36, 3.49, 3.46 3.52 and 3.56 for undoped ZnO, $Zn_{0.97}Mg_{0.03}O$, $Zn_{0.95}Mg_{0.05}O$ and $Zn_{0.93}Mg_{0.07}O$, respectively [19].

3.2. FT-IR Spectral analysis

The chemical functional groups present in undoped ZnO and Mg doped ZnO nanoparticles were confirmed by FT-IR analysis. Fig.3 exhibits a comparison between the FT-IR spectra of the undoped ZnO and the prepared Mg doped ZnO samples using AI gum as bio-template. In all the samples, O–Hstretching appears as a broad band between 3600 and 3200 cm^{-1}.[20] The existence of these bands indicated the existence of absorbed water on the surface of the prepared $Zn_{0.97}Mg_{0.03}O$, $Zn_{0.95}Mg_{0.05}O$ and $Zn_{0.93}Mg_{0.07}O$ nanoparticles.The C-H stretching appears at 2921-2934 cm^{-1} in all the samples. The strong band at 1589 cm^{-1} of pure ZnO is attributed to the C=O stretching of polysaccharides in AI gum. This is shifted towards higher

frequency 1627cm^{-1} side by the addition of Mg dopant. This higher wavenumber shift is due to the slight change in the conformation of the bio-template by the incorporation of Mg as the dopant.

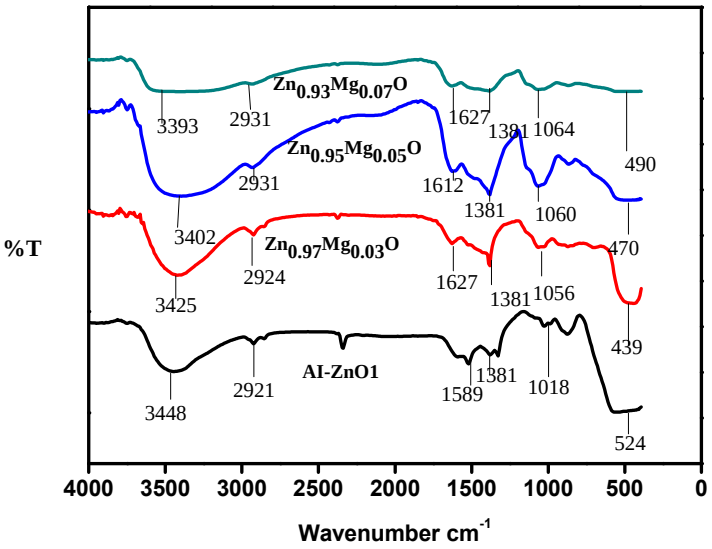

Figure 3: FT-IR Spectra of undoped ZnO and biosynthesized Mg-doped ZnO using AI gum as stabilizing agent.

The peak appears at 1381 cm^{-1} in all the samples is due to C-N stretching vibration and the strong peaks at 1018, 1056, 1064 and 1064 cm^{-1}in ZnO, $Zn_{0.97}Mg_{0.03}O$, $Zn_{0.95}Mg_{0.05}O$ and $Zn_{0.93}Mg_{0.07}O$ nanoparticles indicates the presence of amine groups in AI gum. The presence of peaks at 524,439, 470 and 490 cm^{-1} was the characteristic peaks of Zn-O stretching vibration.[21] The Zn-O peak appears at 524 cm^{-1}in undoped ZnO shifts to lower frequency side (524,439, 470 and 490 cm^{-1}) in Mg doped ZnO due to some structural changes by doping with Mg.

3.3. XRD Analysis

The XRD patterns of the biosynthesized $Zn_{1-x}Mg_xO$ (x= 0.00, 0.03, 0.05 & 0.07) nanoparticles in the 2θ range 20^o- 90^o are shown in Fig-3. All the XRD patterns show strong and more intense diffraction peaks, which are located at the angle of 31.61^o, 34.28^o and 36.1^o which confirm the hexagonal wurtzite structure of Mg-doped ZnO nanoparticles. The observed values are well matched with the standard values JCPDS Card no: 36-1451.

The XRD pattern of Mg-doped ZnO clearly showed that there is a significant shift of diffraction peaks towards the lower angle side, indicating the expansion of a unit cell.[22,23] The shift confirms the replacement of Mg^{2+} into the ZnO matrix in the Zn^{2+} site. This shift is due to the ionic radius of Mg^{2+} ($0.66A^{o}$) is smaller compared to that of Zn^{2+} ($0.74A^{o}$). The intensity of all the diffraction peaks decreases as the doping concentration of Mg increases with peak broadening and there is no additional peak of MgO was observed. This indicates that the presence of Mg concentration in impurity level.

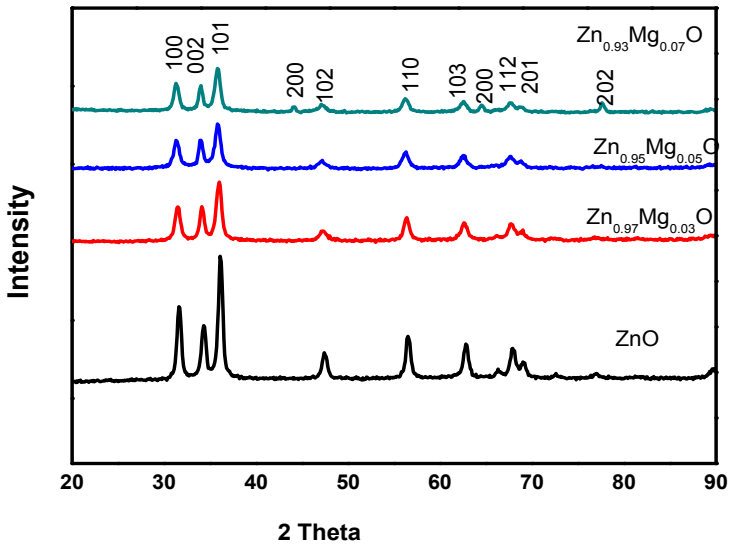

Figure 4: XRD patterns of undoped ZnO and biosynthesized Mg-doped ZnO using AI gum as stabilizing agent.

The average crystallite size of all the prepared undoped and Mg doped ZnO samples are calculated with (101) peak using the Scherer's formula[24],

$$D = \frac{0.9\lambda}{\beta cos\theta}$$

The strain (ε) is calculated using the relation.

$$\varepsilon = \beta \cos\theta /4$$

The dislocation density (δ) defined as the length of dislocation lines per unit volume of the crystal and can be evaluated using the formula.

$$\delta = \frac{1}{D^2}$$

For hexagonal symmetry, the lattice parameters 'a' and 'c' can be determined using the following expression.

$$\frac{1}{d^2} = \frac{4}{3}\frac{h^2+hk+k^2}{a^2} + \frac{l^2}{c^2}$$

The crystallite size, dislocation density and lattice strain and lattice constants 'a', 'c' of the prepared Mg doped and undoped ZnO samples have been calculated and are given in Table .2. The values are in good agreement with the standard JCPDS values (JCPDS card number 36-1451). The strain and dislocation density of the prepared nanoparticles are found to increase with the increase in the doping concentration of Mg.

Table 2: Structural parameters of undoped and Mg doped ZnO nanoparticles synthesized by chemical and green method using AI gum as the stabilizing agent.

S.No	Sample code	Crystallite size (D) (nm)	Lattice Strain (%)	Dislocation density (δ)	Lattice parameters (nm)	
					a	c
1	ZnO	15	0.2310	4.4421	3.276	5.245
2	$Zn_{0.97}Mg_{0.03}O$	13	0.2658	5.880	3.2978	5.2779
3	$Zn_{0.95}Mg_{0.05}O$	11	0.2714	6.132	3.2968	5.2764
4	$Zn_{0.93}Mg_{0.07}O$	11	0.2779	6.42	3.2835	5.2584

3.4. Energy dispersive X- rays analysis

The elemental content in the synthesized sample has been determined with the help of energy dispersive X- ray analysis. The chemical composition of Mg doped ZnO synthesized using AI gum as bio-template has been identified using energy dispersive X- ray analysis and the EDAX pattern (figure 5A, 5B, and 5C). The EDS analysis exhibited clear peaks of only Zn, Mg and O elements, whereas no additional peaks were detected, which means there are no impurities. The percentage of Zn, Mg and O elements present are given in Table.3

Table 3: Elemental composition of Mg doped ZnO nanoparticles.

S.No	Sample code	Zn (at %)	Mg (at %)	Oxygen (at %)
1	$Zn_{0.97}Mg_{0.03}O$	38.63	1.21	60.16
2	$Zn_{0.95}Mg_{0.05}O$	36.06	1.87	62.06
3	$Zn_{0.93}Mg_{0.07}O$	48.06	2.12	49.82

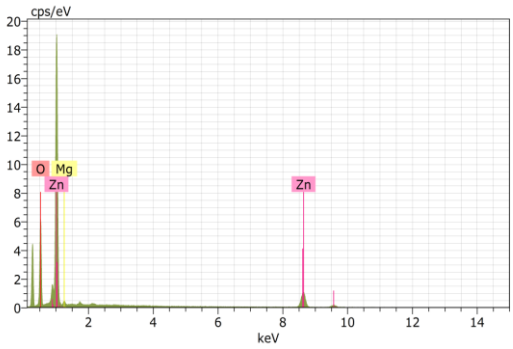

5(A) $Zn_{0.97}Mg_{0.03}O$

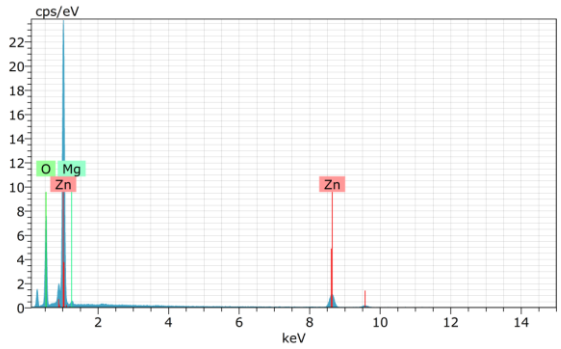

5(B) $Zn_{0.95}Mg_{0.05}O$

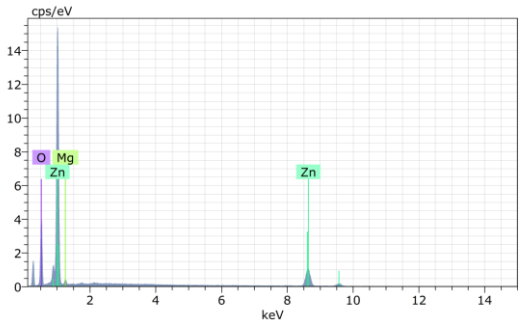

5(C) $Zn_{0.93}Mg_{0.07}O$

Figure.5A, 5B, and 5C EDAX spectra of Mg doped ZnO nanoparticles.

3.5. FE-SEM analysis

Fig.6 shows the Field Emission Scanning Electron Microscope (FE-SEM) image of Mg doped ZnO nanoparticles. Flower like structure were found for all the three Mg ZnO nanoparticles and also it is found that particles was closely packed while increasing the concentration of Mg. FE-SEM image clearly shows that Mg doped ZnO nanoparticles show uniform spherical shape with nearly flower shape structure.

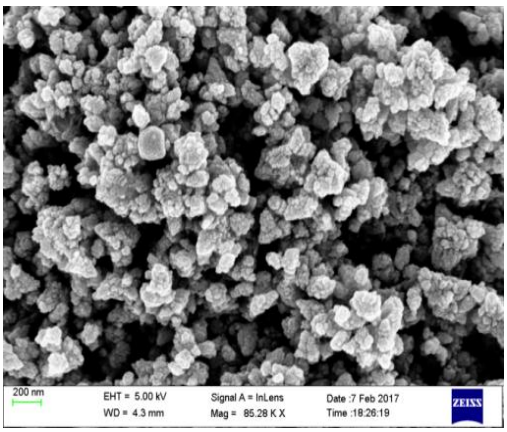

6(a) $Zn_{0.97}Mg_{0.03}O$

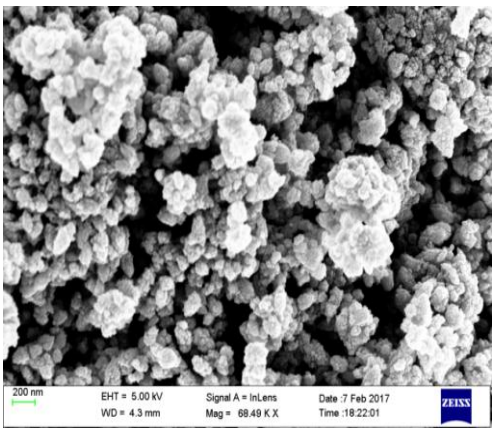

6(b) $Zn_{0.95}Mg_{0.05}O$

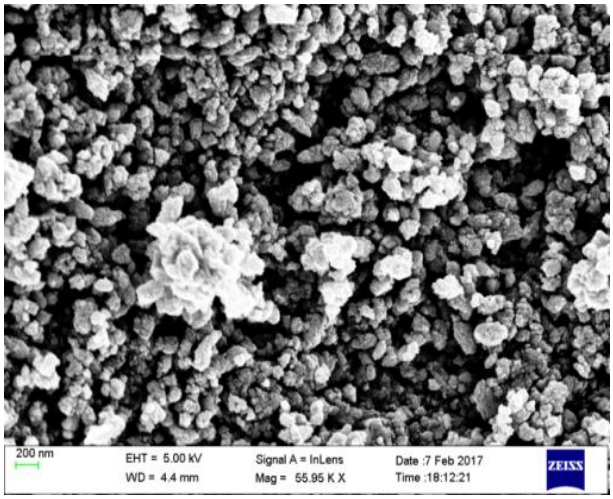

6(c) $Zn_{0.93}Mg_{0.07}O$

Figure 6: Field Emission SEM images of Mg-ZnO nanoparticles (a) $Zn_{0.97}Mg_{0.03}O$ (b)$Zn_{0.95}Mg_{0.05}$ and (c) $Zn_{0.93}Mg_{0.07}O$.

3.6. Antibacterial assay

The special features of nanoparticles are the larger surface to volume ratio renders greater surface area of contact with the bacterial pathogens and enhanced its reactivity. The smaller size of the Mg doped ZnO nanoparticles facilitates easy entry into the microbial cell membrane and inside the cell, it generates hydrogen peroxide which chemically reacts with.

Table 4: Zone of inhibition of Mg doped ZnO nanoparticles.

S.No	Sample code	Zone of inhibition(mm)	
		E. coli	*S. aureus*
1	$Zn_{0.97}Mg_{0.03}O$	11	17
2	$Zn_{0.95}Mg_{0.05}O$	14	20
3	$Zn_{0.93}Mg_{0.07}O$	22	23

The bacterial strains and induces cell death. From table.4 the maximum zone of inhibition was observed in $Zn_{0.93}Mg_{0.07}O$ of about 22 mm against *E.coli* and 23 mm against *S.aureus*. The $Zn_{0.95}Mg_{0.05}O$ exhibits the higher zone of inhibition of about 14 mm against *E.coli* and 20 mm against *S.aureus*. The least zone of inhibition was revealed in $Zn_{0.97}Mg_{0.03}O$ about 11 mm and 17 mm against *E. coli* and *S. aureus* respectively.

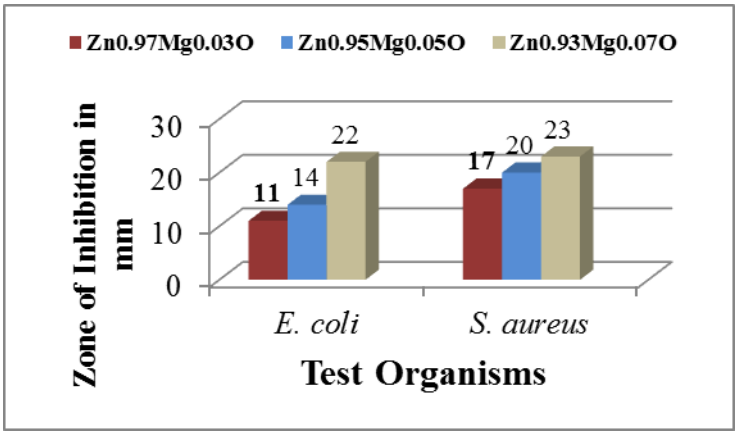

Figure.7 Antibacterial activity of Mg-ZnO nanoparticles (a) $Zn_{0.97}$ $Mg_{0.03}$ O (b)$Zn_{0.95}$ $Mg_{0.05}$ and (c) $Zn_{0.93}$ $Mg_{0.07}$ O

CONCLUSION

The zinc oxide nanoparticles with different Mg concentration $Zn_{0.97}$ $Mg_{0.03}$ O, $Zn_{0.95}$ $Mg_{0.05}$ and $Zn_{0.93}$ $Mg_{0.07}$ O were green synthesized by the wet chemical method using AI gum as the stabilizing agent (bio-template). The nanocrystalline hexagonal structure was revealed by XRD with a preferred hexagonal wurzite structure and the lattice constants ‘a’ and ‘c’ values were also calculated and well matched with JCPDS Card no 36-1451. The elemental composition of the synthesized nanoparticles was determined by EDAX which confirmed the presence of elements Zn, Mg and O. The band gap energy of the Mg doped ZnO nanoparticles were found to increase with the increase in Mg concentration. The FE-SEM shows uniformity in particle size with nearly flower shape morphology. The antibacterial activity results proved the as-green synthesized Mg doped ZnO nanoparticles can be used as a safe antimicrobial agent and also used as a photo catalyst in various applications.

REFERENCES

1. Surendiran A, Sandhiya S, Pradhan SC and Adithan C, Novel applications of nanotechnology in medicine, Indian Journal of Medical Research, 2009; 130: 689-701.
2. Sabir S, Arshad S and Chaudari SK, Zinc oxide nanoparticle for Revolutionizing Agriculture: Synthesis and Application, The Scientific World Journal, article ID 925494, 2014; 8 pages http://dx.doi.org/10.1155/2014/925494.
3. Hartini Ahmad Rafaie, Roslan Md. Nor and YusoffMohd Amin, Magnesium doped ZnO nanostructures synthesis using *citrus aurantifolia*extracts: Structural and field electron emission properties, Materials Express, 2015; 5(3): 226-232.

4. Sharma M and Jeevanandam P, Synthesis, characterization and studies on optical properties of indium doped ZnO Nanoparticles, Indian Journal of Chemistry, 2014; 53A: 561-565.
5. Amna Sirelkhatim, Shahrom Mahmud, Azman Seeni, Noor Haida Mohamad Kaus, and Dasmawati Mohamad, Review on Zinc oxide nanoparticle: Antibacterial activity and toxicity mechanism, Nano Micro letter, 2015; 7(3): 219-242.
6. Renata Dobrucka and Jolanta Dugaszewska B, Biosynthesis and antibacterial activity of ZnO nanoparticles using *Trifolium pratense* flower extract, Saudi Journal of Biological Sciences, 2016; 23: 517-523.
7. Bing-Lei Guo, Ping Han, Li-Chuan Guo, Yan-Qiang Cao, Ai-Dong Li, Ji-Zhou Kong, Hai-Fa Zhai and Di Wu, The Antibacterial Activity of Ta-doped ZnO Nanoparticles, Springer: Nanoscale research letter, 2015; 10: 336.
8. Viswanathan R, Venkatesh TG, Vidyasagar CC and Arthoba Nayaka Y, Preparation and Characterization of ZnO and Mg-ZnO nanoparticle, Scholars Research Library, (2012); 4(1): 480-486.
9. Jafar Ahamed A, Vijaya Kumar P and Karthikeyan M, Synthesis, structural and antibacterial properties of Mg Doped ZnO Nanoparticles, Journal of Environmental Nanotechnology, 2016; 5(2): 11-16.
10. Maddahi P, Shahtahmasebi N, Kompany A, Mashreghi M, Safaee S and Roozban F Effect of doping on structural and optical properties of ZnO nanoparticles: study of antibacterial properties, Material Science Poland, 2014; 32(2): 130-135.
11. Qiu X, Li L, Zheng J, Liu J, Sun X, Li G, J. Phys. Chem. C, 2008; 112: 12242-12248.
12. Aruna Jyothi Koraa, R.B, Sashidharb and Arunachalam J, Process Biochemistry, 2012; 47: 1516–1520.
13. Vijaya Kattumuri, Kavita Katti, Sharanya Bhaskaran, Evan J. Boote, Stan W. Casteel, Raghuraman Kannan, and Kattesh V. Katti, Nanomedicine, 2007; 3(2): 333-341.
14. Aruna Jyothi Kora, Sashidhar RB and Arunachalam J, Carbohydrate Polymers, 2010; 82: 670–679.
15. Vinod Vellora Thekkae Padil and Miroslav Černík, International Journal of Nanomedicine, 2013; 8: 889-897.
16. Keerthi Devi D, Veera Pratap S, Haritha R, Samba Sivudu K, Radhika P, and Sreedhar B, Journal of Applied Polymer Science, 2011; 121: 1765–1773.

17. A.Geetha, R.Sakthivel and J.Mallika, Green Synthesis of Antibacterial Zinc Oxide Nanoparticles Using Biopolymer *Azadirachta indica* Gum, Oriental journal of chemistry, 2016; 32(2).
18. Geetha A, Sakthivel R and Mallika J, A Single pot green synthesis of ZnO nanoparticles using aqueous gum exudates of *Azadirachta indica* and its antifungal activity, International research journal of engineering and technology, 2016; 3(9): 301-306.
19. Hui li, Yongzhe Zhang , Xiaojun Pan, Hongliang Zhang Tao Wang, and Erqing Xie, Effects of In and Mg doping on properties of ZnO nanoparticles by flame spray synthesis, J Nanopart Res, 2009; 11: 917–921.
20. Guang-Hui Ning, Xiao-Peng Zhao, Jia Li, Structure and optical properties of $Mg_xZn_{1-x}O$ nanoparticles prepared by sol–gel method, Opt. Mater, 2004; 27: 1–5.
21. Jimenez Gonzalez AE, Soto Urueta J.A, Suarez Parra R, J. Cryst. Growth, 1998; 192: 430.
22. Vijayalakshmi K, Karthick K, Influence of annealing on the Photoluminescence of nanocrystalline ZnO synthesized by micro-wave processing, Philos. Mag. Lett, 2012; 92(12): 710–717.
23. Clament Sagaya Selvam N, Narayanan S, John Kennedy L and Judith Vijaya J, Pure and Mg-doped self-assembled ZnO nano-particles for the enhanced photo catalytic degradation of 4-chlorophenol, Journal of Environmental Sciences, 2013; 25(10): 2157–2167.
24. B.D. Cullity, Elements of X-ray Diffractions, Addison-Wesley, Reading, MA, 1978; 102.